Demonstration of ISCO Treatment of a DNAPL Source Zone at Launch Complex 34 in Cape Canaveral Air Station

Final Innovative Technology Evaluation Report

Prepared for

The Interagency DNAPL Consortium:

U.S. Department of Energy
U.S. Environmental Protection Agency
U.S. Department of Defense
National Aeronautics and Space Administration

Prepared by

Battelle
505 King Avenue
Columbus, OH 43201

October 17, 2002

Appendix A

Performance Assessment Methods

A.1 Statistical Design and Data Analysis Methods

Estimating TCE/DNAPL mass removal due to the in situ chemical oxidation (ISCO) technology application was a critical objective of the IDC demonstration at Launch Complex 34. Analysis of TCE in soil samples collected in the ISCO plot before and after the demonstration was the main tool used to make a determination of the mass removal. Soil sampling was used to obtain pre- and postdemonstration data on the TCE distribution in the ISCO plot. Three data evaluation methods were used for estimating TCE/DNAPL masses in the ISCO plot before and after the demonstration:

- Linear interpolation by contouring
- Kriging

Section 4.1 (in Section 4.0 of the report) contains a general description of these two methods. Section 5.1 (in Section 5.0 of this report) summarizes the results.

The *contouring* method is the most straightforward and involves determining TCE concentrations at unsampled points in the plot by linear interpolation (estimation) of the TCE concentrations between sampled points. The contouring software EarthVision™ uses the same methodology that is used for drawing water level contour maps based on water level measurements at discrete locations in a region. The only difference with this software is that the TCE concentrations are mapped in three dimensions to generate iso-concentration shells. The TCE concentration in each shell is multiplied by the volume of the shell (as estimated by the software) and the bulk density of the soil (1.59 g/cc, estimated during preliminary site characterization) to estimate a mass for each shell. The TCE mass in each region of interest (Upper Sand Unit, Middle-Fine-Grained Unit, Lower Sand Unit, and the entire plot) is obtained by adding up the portion of the shells contained in that region. The DNAPL mass is obtained by adding up the masses in only those shells that have TCE concentrations above 300 mg/kg. Contouring provides a single mass estimate for the region of interest.

The contouring method relies on a high sampling density (collecting a large number of samples in the test plot) to account for any spatial variability in the TCE concentration distribution. By collecting around 300 samples in the plot during each event (before and after treatment) the expectation is that sufficient coverage of the plot has been obtained to make a reliable determination of the true TCE mass in the region of interest. Section A.1.1 of this appendix describes how the number of samples and appropriate sampling locations were determined to obtain good coverage of the 75 ft x 50 ft plot.

Kriging is a statistical technique that goes beyond the contouring method described above and addresses the spatial variability of the TCE distribution by taking into account the uncertainties associated with interpolating between sampled points. Unlike contouring, which provides a single mass estimate, Kriging provides a range of estimated values that take into account the uncertainties (variability) in the region of interest. Section A.1.2 describes the kriging approach and results

A.1.1 Sampling Design to Obtain Sufficient Coverage of the ISCO plot

Selection of the sampling plan for this particular test plot was based, in part, on the objectives of the study for which the samples were being collected. In this study, the objectives were:

- **Primary objective:** To determine the magnitude of the reduction in the levels of TCE across the entire test plot.

- **Secondary objectives:**

  - To determine whether remediation effectiveness differs by depth (or stratigraphic unit such as the upper sand unit [USU], middle fine-grained unit [MFGU], or lower sand unit [LSU]).
  - To determine whether the three remediation technologies demonstrated differ in their effectiveness at removing chlorinated volatile organic compounds (CVOCs).

Four alternative plans for selecting the number and location of sampling in the test plot were examined. These four plans were designated as simple random sampling (SRS), paired sampling, stratified sampling, and systematic sampling. Each plan is discussed in brief detail below.

Simple Random Sampling

The most basic statistical sampling plan is SRS, in which all locations within a given sampling region are equally likely to be chosen for sampling. For this study, using SRS would require developing separate SRS plans for each of the three test plots. In addition, because two sampling events were planned for the test plot, using SRS would involve determining two sets of unrelated sampling locations for the test plot.

The main benefit of using SRS is that the appropriate sample size can be determined easily based on the required power to detect a specific decrease in contaminant levels. In addition, SRS usually involves a reasonable number of samples. However, a key disadvantage of using SRS is that it would not guarantee complete coverage of the test plot; also, if contaminant levels are spatially correlated, SRS is not the most efficient sampling design available.

Paired Sampling

Paired sampling builds on SRS methods to generate one set of paired sampling locations for a given test plot rather than two separate sets. Instead of sampling from each of two separate random sample locations for pre- and post-remediation sampling, paired sampling involves the positioning of post-remediation sample locations near the locations of pre-remediation sampling. The number of samples required to meet specific power and difference requirements when using this design would be similar to the number of locations involved using SRS; the exact sample size cannot be determined because information is required about contaminant levels at collocated sites before and after remediation.

Paired sampling offers three significant benefits to this particular study. First, the work of determining the sampling locations is reduced in half. Second, the comparison of contaminant

levels before and after remediation is based on the differences in levels at collocated sites. Third, the variability of the difference should be less than the variability associated with the SRS, which would result in a more accurate test. The disadvantages of this sampling procedure are the same as with the SRS: there is no guarantee of complete coverage of the test plot, and the plan is inefficient for spatially correlated data.

Stratified Sampling

Stratified sampling guarantees better coverage of the plot than either SRS or paired sampling: to ensure complete coverage of a given test plot, it is divided into a regular grid of cells, and random samples are drawn from each of the grid cells. Samples then are selected within each grid cell either using SRS or paired sampling. The number of samples required to meet specific power and difference requirements would be slightly greater than that for SRS, although the difference would not be great. For this study, which involves test plots 50 × 75 ft in size, the most effective grid size would be 25 × 25 ft, which results in six grid cells per test plot.

Again, the main benefit of stratified sampling is that it guarantees more complete coverage of the test plot than SRS or paired sampling. Also, if any systematic differences in contaminant levels exist across the site, stratified sampling allows for separate inferences by sub-plot (i.e., grid cell). Disadvantages of stratified sampling are that the method requires a slightly larger number of samples than SRS or paired sampling methods, and that stratified sampling performs poorly when contaminant levels are spatially correlated.

Systematic Sampling

The samples for the ISCO techonology demonstration were collected using a systematic sampling plan. Systematic sampling is the term applied to plans where samples are located in a regular pattern. In geographic applications such as this study, the systematic sampling method involves the positioning of sampling locations at the nodes of a regular grid. The grid need not be square or rectangular; in fact, a grid of equilateral triangles is the most efficient grid design. (Regular hexagonal grids also have been used regularly and are nearly as efficient as triangles and squares.) The number of samples and the size of the area to be sampled determine the dimensions of the grid to be used. With systematic sampling, the selection of initial (e.g., pre-remediation) set of sampling locations requires the random location of only one grid node, because all other grid nodes will be determined based on the required size of the grid and the position of that first node. A second (e.g., post-remediation) set of sampling locations can be either chosen using a different random placement of the grid or collocated with the initial set of sampling locations.

One variation of the systematic sampling method worth consideration is *unaligned* sampling. Under this method, a given test plot is divided into a grid with an equal number of rows and columns. One sample per grid cell then is selected by:

- Assigning random horizontal coordinates for each row of the grid;
- Assigning random vertical coordinates for each column of the grid;
- Determining the sampling locations for a cell by using the horizontal and vertical coordinates selected for the corresponding row and column.

In other words, every cell in a row shares a horizontal coordinate, and every cell in a column shares a vertical coordinate. Figure A-1 illustrates the locations generated using unaligned systematic sampling with a 3 × 3 grid.

The major benefit of systematic sampling was that it is the most efficient design for spatially correlated data. In addition, coverage of the entire plot was guaranteed. One disadvantage of systematic sampling was that determining the required sample size was more difficult than the other three methods discussed in this appendix.

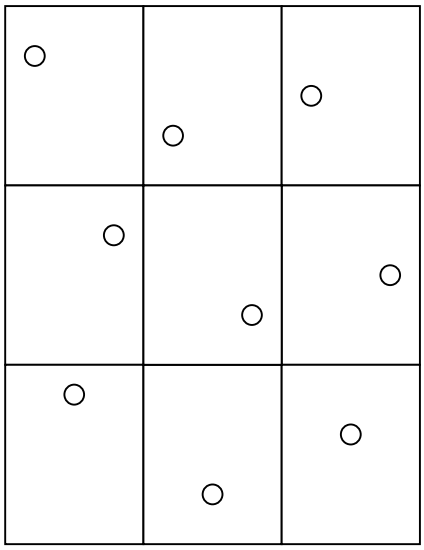

Figure A.1-1. Unaligned Systematic Sampling Design for a 3 × 3 Grid

A.1.2 Kriging Methods and Results

The geostatistical analysis approach was to utilize kriging, a statistical spatial interpolation procedure, to estimate the overall average TCE concentration in soil before and after remediation, and then determine if those concentrations were significantly different.

To meet the objectives of this study, it is sufficient to estimate the overall mean TCE concentration across an entire test plot, rather than estimating TCE concentrations at various spatial locations within a test plot. In geostatistical terms, this is known as global estimation. One approach, and in fact the simplest approach, for calculating a global mean estimate is to calculate the simple arithmetic average (i.e., the equally weighted average) across all available TCE concentrations measured within the plot. However, this approach is appropriate only in cases where no correlation is present in the measured data. Unfortunately, this is a rare situation in the environmental sciences.

A second approach, and the approach taken in this analysis, is to use a spatial statistical procedure called kriging to take account of spatial correlation when calculating the global average. Kriging is a statistical interpolation method for analyzing spatially varying data. It is used to estimate TCE concentrations (or any other important parameter) on a dense grid of spatial locations covering the region of interest, or as a global average across the entire region. At each location, two values are calculated with the kriging procedure: the estimate of TCE concentration (mg/kg), and the standard error of the estimate (also in mg/kg). The standard error can be used to calculate confidence intervals or confidence bounds for the estimates. It should be noted that this

calculation of confidence intervals and bounds also requires a serious distributional assumption, such as a normality assumption, which is typically more reasonable for global estimates than for local estimates.

The kriging approach includes two primary analysis steps:

1. Estimate and model spatial correlations in the available monitoring data using a semivariogram analysis.
2. Use the resulting semivariogram model and the available monitoring data to interpolate (i.e., estimate) TCE values at unsampled locations; calculate the statistical standard error associated with each estimated value.

A.1.2.1 Spatial Correlation Analysis

The objective of the spatial correlation analysis is to statistically determine the extent to which measurements taken at different locations are similar or different. Generally, the degree to which TCE measurements taken at two locations are different is a function of the distance and direction between the two sampling locations. Also, for the same separation distance between two sampling locations, the spatial correlation may vary as a function of the direction between the sampling locations. For example, values measured at each of two locations, a certain distance apart, are often more similar when the locations are at the same depth, than when they are at the same distance apart but at very different depths.

Spatial correlation is statistically assessed with the semivariogram function, (($\underline{h}$), which is defined as follows (Journel and Huijbregts, 1981):

$$2(\ (\underline{h}) = E\ \{[Z(\underline{x}) - Z(\underline{x} + \underline{h})]^2\}$$

where $Z(\underline{x})$ is the TCE measured at location $\underline{x}$, $\underline{h}$ is the vector of separation between locations $\underline{x}$ and $\underline{x} + \underline{h}$, and E represents the expected value or average over the region of interest. Note that the location $\underline{x}$ is typically defined by an easting, northing, and depth coordinate. The vector of separation is typically defined as a three-dimensional shift in space. The semivariogram is a measure of spatial differences, so that small semivariogram values correspond to high spatial correlation, and large semivariogram values correspond to low correlation.

As an initial hypothesis, it is always wise to assume that the strength of spatial correlation is a function of both distance and direction between the sampling locations. When the spatial correlation is found to depend on both separation distance and direction, it is said to be anisotropic. In contrast, when the spatial correlation is the same in all directions, and therefore depends only on separation distance, it is said to be isotropic.

The spatial correlation analysis is conducted in the following steps using the available measured TCE data:

- Experimental semivariogram curves are generated by organizing all pairs of data locations into various separation distance and direction classes (e.g., all pairs separated by 20-25 ft. in the east-west direction $\forall$ 22.5º), and then calculating within each class the average squared-difference between the TCE measurements taken at each pair of locations. The results of these calculations are plotted against separation distance and by separation direction.

- To help fully understand the spatial correlation structure, a variety of experimental semivariogram curves may be generated by subsetting the data into discrete zones, such as different depth horizons. If significant differences are found in the semivariograms they are modeled separately; if not, the data are pooled together into a single semivariogram.
- After the data have been pooled or subsetted accordingly, and the associated experimental semivariograms have been calculated and plotted, a positive-definite analytical model is fitted to each experimental curve. The fitted semivariogram model is then used to input the spatial correlation structure into the subsequent kriging interpolation step.

A.1.2.2 Interpolation Using Ordinary Kriging

Ordinary kriging is a linear geostatistical estimation method which uses the semivariogram function to determine the optimal weighting of the measured TCE values to be used for the required estimates, and to calculate the estimation standard error associated with the estimates (Journel and Huijbregts, 1981). In a sense, kriging is no different from other classical interpolation and contouring algorithms. However, kriging is different in that it produces statistically optimal estimates and associated precision measures. It should be noted that the ordinary kriging variance, while easy to calculate and readily available from most standard geostatistical software packages, may have limited usefulness in cases where local estimates are to be calculated, and the data probability distribution is highly skewed or non-gaussian. The ordinary kriging variance is more appropriately used for global estimates and symmetric or gaussian data distributions. The ordinary kriging variance provides a standard error measure associated with the data density and spatial data arrangement relative to the point or block being kriged. However, the ordinary kriging variance is independent of the data values themselves, and therefore may not provide an accurate measure of local estimation precision.

A.1.2.3 TCE Data Summary

Semivariogram and kriging analyses were conducted on data collected from two test plots; one plot used ISCO technology, and the other used a standard Resistive Heating technology to remove TCE. Each plot was approximately 50 by 75 feet in size, and was sampled via 25 drill holes, half before and half after remediation. The location of each drill hole was recorded by measuring the distance in the northing and easting directions from a designated point on the Cape Canaveral Air Station. The documented coordinates for each drill hole on the ISCO and Resistive Heating plots are defined within Figure A.1-2. The same locations are also shown in Figure A.1-3 after we rotated both plots by 30 degrees and shifted the coordinates in order to produce a posting map that was compatible with the kriging computer software.

Each point within Figures A.1-2 and A.1-3 represents a single drill hole. Recall that pre- and post-remediation TCE measurements were collected in order to analyze the effectiveness of the contaminant removal methods. Thus, the drill holes were strategically placed so that pre and post information could be gathered within a reasonable distance of one another (i.e., the holes were approximately paired). In addition, for both the ISCO and the Resistive Heating plots, an extra or twinned post-remediation hole was drilled (see pre/post pair # 10B and 17B on Figures A.1-2 and A.1-3). Since our approach for the kriging analysis considered the pre- and post-remediation data as independent data sets (see Section 1.0), we included the duplicate holes in our analyses, even though a corresponding pre-remediation hole did not exist.

The cores were drilled at least 44 feet deep; and the largest drill hole extends 48 feet. With few exceptions, TCE measurements were collected every two feet. Thus, approximately 20 to 25 two-foot core sections were analyzed from each drill hole. The vertical location of each core section was identified by the elevation of the midpoint of the section above sea level. At the time of data collection, the surface elevation at the location of the drill hole, as well as the top and bottom depths of each core section (rounded to the nearest half of a foot), were recorded. Hence, the elevation of each sample was calculated by the subtracting the average of the top and bottom depths from the surface elevation. For example, if a sample was collected from a core section that started and ended at 20 and 22 feet below a ground surface elevation of 5.2 feet, then the sample elevation equaled 5.2 - (20+22)/2=15.8 feet above sea level.

In some cases, field duplicate samples were collected by splitting an individual two-foot core section. In order to optimize the additional data, we used all measurements when evaluating spatial correlation with the semivariogram analysis, and when conducting the kriging analysis. However, to remain compatible with the kriging software, it was necessary to shift the location of the duplicate data slightly, by adding one-tenth of a foot to the easting coordinate. Table A.1-1 summarizes the number of two-foot sections from which more than one sample was collected.

Table A.1-1. Number of Field Duplicate Measurements Collected from the Resistive Heating and ISCO Plots

Plot	Pre/Post	Number of Two-Foot Sections From Which		Total
		1 Sample was Drawn	> 1 Sample was Drawn	
Resistive Heating	Pre	242	20	262
	Post	246	28	292
ISCO	Pre	251	16	267
	Post	276	12	288

There were also cases where the observed TCE concentration for a particular sample occurred below the analytical method detection limit (MDL). In such cases, the measurement that was included in our analyses equaled one-half of the given MDL. Table A.1-2 summarizes the number of observations that were below the MDL.

Table A.1-2. Number of Measurements (including Duplicates) Below the Minimum Detection Limit

Plot	Pre/Post	Number of Samples		Total
		Below MDL	Above MDL	
Resistive Heating	Pre	47	231	278
	Post	29	276	305
ISCO	Pre	20	266	286
	Post	156	144	300

When a two-foot section was removed from the core, the sample was identified by the easting, northing, and elevation coordinates. In addition, the geologic stratum, or soil type of the sample, was also documented. These strata and soil types included the vadose zone, upper sand unit (USU), middle fine-grained unit (MFGU), and lower sand unit (LSU). Note that the stratum of the sample was not solely determined by depth, but also by inspection by a geologist.

Tables A.1-3 and A.1-4 provide summary statistics by layer and depth for pre- and post-remediation measurements. The minimum and maximum values provide the overall range of the data; the mean or average TCE measurement estimates (via simple arithmetic averaging) the amount of TCE found within the given layer and depth; and the standard deviation provides a sense of the overall spread of the data. Note that our analyses focus on the three deepest layers, USU, MFGU and LSU.

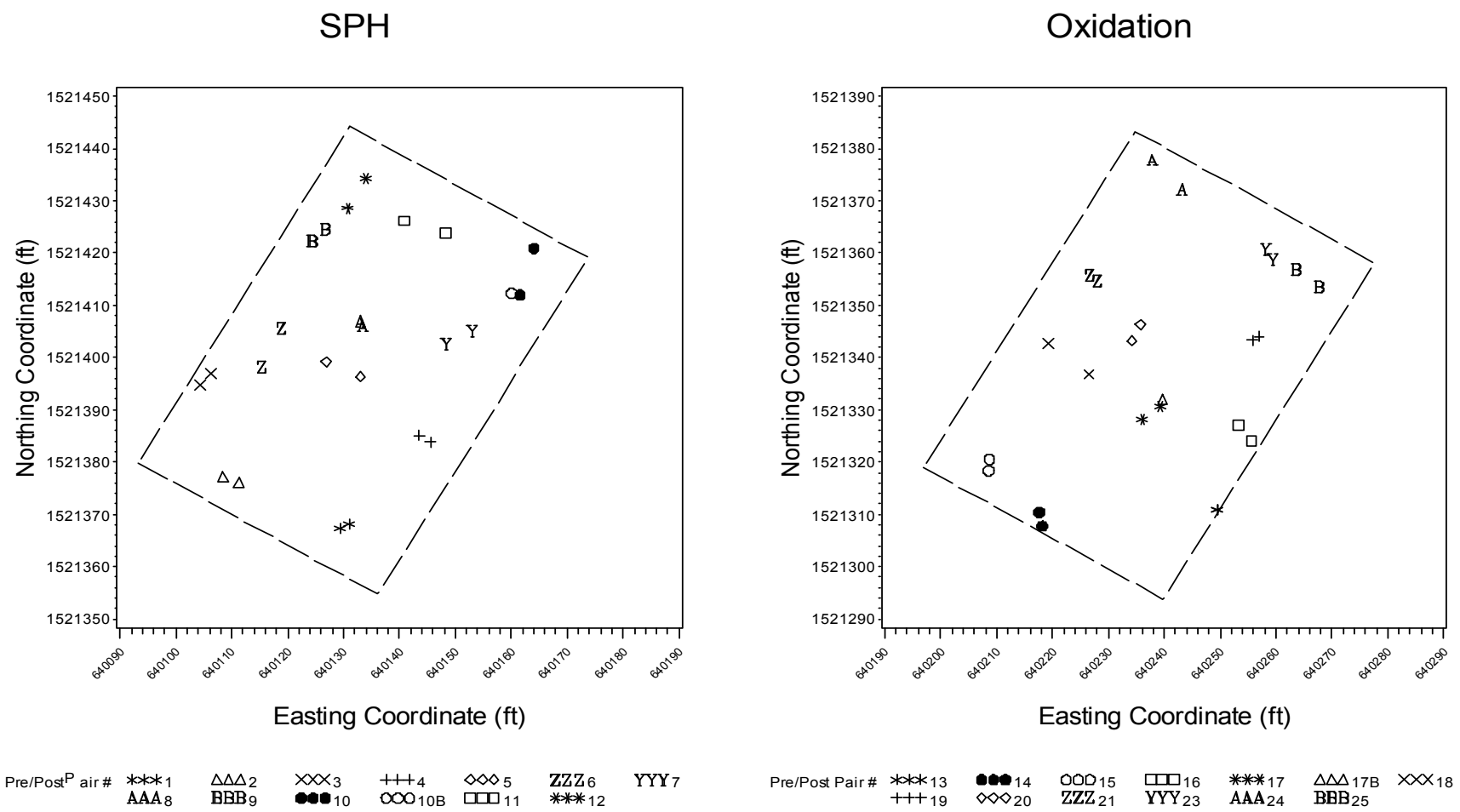

Figure A.1-2. Original Posting Maps of Resistive Heating (SPH) and ISCO plots
(Note that pre/post pair # 13 has two drill holes that are extremely close to one another)

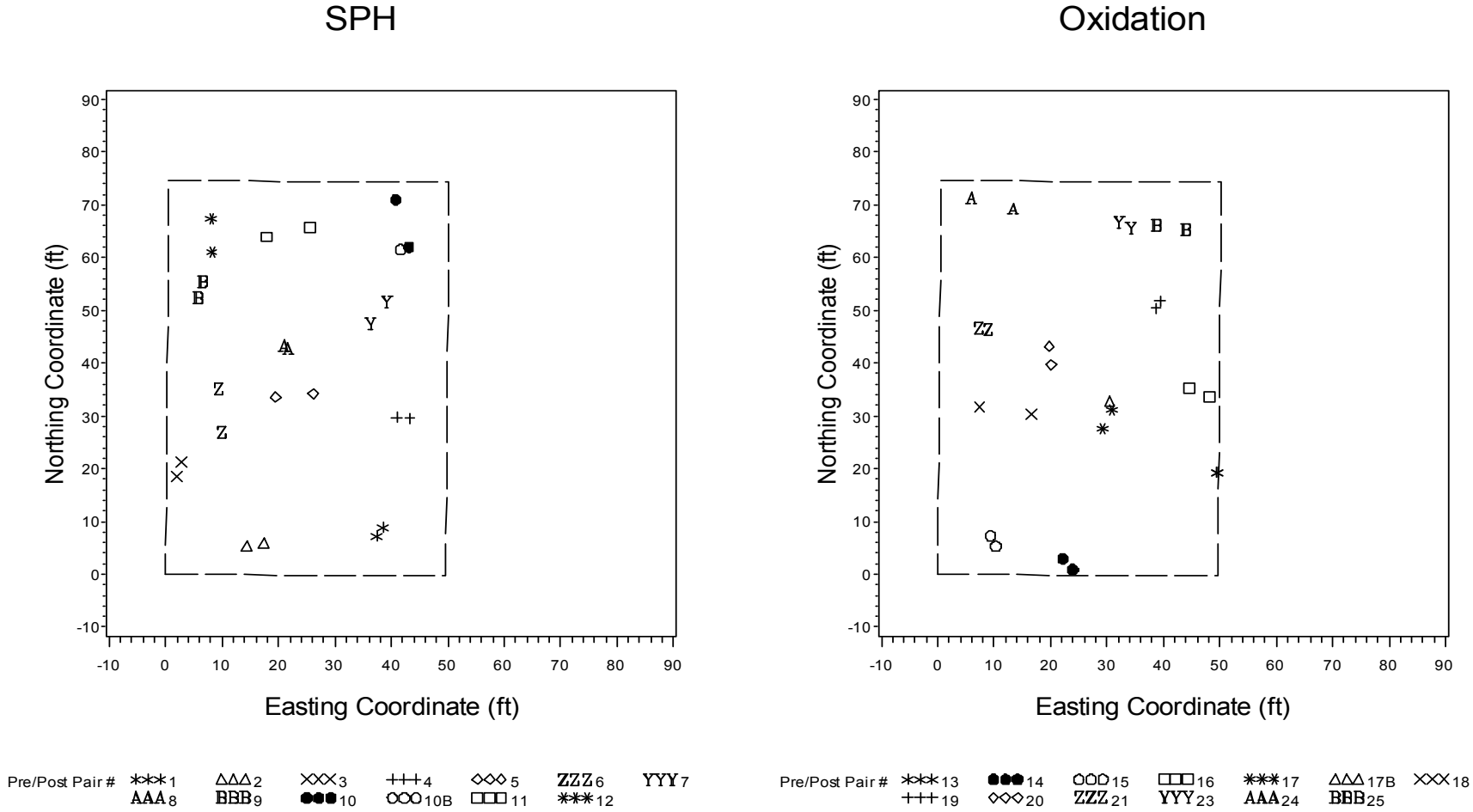

Figure A.1-3. Rotated Posting Maps of Resistive Heating (SPH) and ISCO plots
(Note that pre/post pair # 13 has two drill holes that are extremely close to one another)

Table A.1-3. Summary Statistics for Data Collected From Resistive Heating Plot by Layer and Depth

Layer	Feet Above Sea Level (MSL)	Pre-Treatment					Post-Treatment				
		N	Minimum (mg/kg)	Maximum (mg/kg)	Mean (mg/kg)	Std. Dev. (mg/kg)	N	Minimum (mg/kg)	Maximum (mg/kg)	Mean (mg/kg)	Std. Dev. (mg/kg)
VADOSE	10 to 12	1	7.78	7.78	7.78	.	2	0.26	0.77	0.51	0.36
	8 to 10	1	5.29	5.29	5.29	.	6	0.25	6.00	2.67	2.62
	6 to 8	6	0.14	9.24	2.01	3.59	12	0.25	6.00	1.84	1.77
	4 to 6	12	0.14	4.63	1.25	1.63	13	0.21	12.00	2.61	3.53
	2 to 4	12	0.10	10.52	1.75	3.16	13	3.00	40.22	9.32	11.22
	0 to 2	10	0.17	48.74	5.26	15.29	3	10.00	72.00	47.67	33.08
	-2 to 0	2	0.20	1.10	0.65	0.64	.	.	.	.	.
	Total	44	0.10	48.74	2.61	7.55	49	0.21	72.00	6.88	14.23
USU	0 to 2	2	0.71	8.84	4.77	5.75	10	5.00	90.00	30.31	27.06
	-2 to 0	9	0.18	12.46	2.27	4.06	12	0.22	114.00	20.85	35.55
	-4 to -2	11	0.18	6.46	1.65	2.09	9	0.22	71.00	18.84	27.65
	-6 to -4	10	0.18	4.01	1.05	1.24	12	0.16	126.00	36.26	47.60
	-8 to -6	13	0.17	121.67	10.73	33.41	12	0.26	197.00	50.52	72.10
	-10 to -8	13	0.20	341.80	51.64	122.88	13	1.00	4295.43	358.08	1183.66
	-12 to -10	11	0.19	1935.01	182.22	581.52	11	0.17	1248.08	154.42	368.78
	-14 to -12	12	0.20	107.82	22.01	32.52	11	5.00	135.00	62.56	45.67
	-16 to -14	10	9.20	1835.15	224.50	569.37	10	4.00	213.00	96.89	80.34
	-18 to -16	5	10.77	259.76	86.43	101.53	2	6.00	64.00	35.00	41.01
	-20 to -18	2	26.27	112.13	69.20	60.71	1	20.00	20.00	20.00	.
	Total	98	0.17	1935.01	60.75	271.45	103	0.16	4295.43	95.78	437.80
MFGU	-14 to -12	1	820.43	820.43	820.43	.	1	3927.05	3927.05	3927.05	.
	-16 to -14	2	292.17	526.14	409.16	165.45	5	12.00	401.30	252.87	150.23
	-18 to -16	5	183.22	9050.90	2192.46	3844.52	12	4.00	5560.77	704.64	1539.34
	-20 to -18	13	26.37	19090.91	3314.22	6670.74	12	13.00	403.00	215.36	159.67
	-22 to -20	10	54.64	541.79	196.80	148.15	8	10.00	319.00	131.66	102.29
	-24 to -22	8	17.00	11085.00	1533.59	3871.12	4	7.00	140.00	55.25	61.99
	-26 to -24	3	2.24	5345.08	1783.27	3084.62	2	3.00	19.00	11.00	11.31
	-28 to -26	2	0.39	0.39	0.39	0.00	2	5.00	23.00	14.00	12.73
	-30 to -28	2	0.20	1.40	0.80	0.85	2	1.00	1.00	1.00	0.00
	-32 to -30	1	0.68	0.68	0.68	.	1	3.00	3.00	3.00	.
	Total	47	0.20	19090.91	1601.61	4152.73	49	1.00	5560.77	358.38	942.46
LSU	-20 to -18	.	.	.	.	.	1	1217.00	1217.00	1217.00	.
	-22 to -20	3	34.76	349.12	186.05	157.51	5	34.00	464.64	233.38	158.60
	-24 to -22	6	4.79	623.63	176.84	231.51	10	20.70	287.00	139.97	101.17
	-26 to -24	9	0.18	1024.58	213.91	332.94	11	35.00	429.15	192.80	145.10
	-28 to -26	11	0.28	23361.76	4599.56	8705.84	12	63.00	473.85	279.32	148.04
	-30 to -28	10	0.23	8061.67	1430.78	2922.44	12	2.00	264.00	143.55	86.98
	-32 to -30	9	0.21	28167.63	3338.38	9314.75	11	9.00	335.08	123.18	107.14
	-34 to -32	12	0.43	33099.93	3357.69	9549.49	12	0.17	511.00	167.27	179.23
	-36 to -34	12	5.75	41043.56	7635.34	15205.72	12	0.19	364.00	144.99	126.21
	-38 to -36	12	11.76	37104.00	6980.34	12891.67	3	2.00	59.00	23.00	31.32
	-40 to -38	1	1.46	1.46	1.46	.	.	.	.	.	.
	Total	85	0.18	41043.56	3696.17	9459.97	89	0.17	1217.00	181.46	176.47

Table A.1-4. Summary Statistics for Data Collected From ISCO Plot by Layer and Depth

Layer	Feet Above Sea Level (MSL)	Pre-Treatment					Post-Treatment				
		N	Minimum (mg/kg)	Maximum (mg/kg)	Mean (mg/kg)	Std. Dev. (mg/kg)	N	Minimum (mg/kg)	Maximum (mg/kg)	Mean (mg/kg)	Std. Dev. (mg/kg)
VADOSE	10 to 12	2	0.16	0.20	0.18	0.03	2	0.15	0.40	0.28	0.18
	8 to 10	4	0.13	0.37	0.26	0.11	13	0.15	0.55	0.35	0.14
	6 to 8	12	0.15	4.72	0.68	1.28	13	0.10	0.60	0.31	0.16
	4 to 6	12	0.17	1.81	0.52	0.47	13	0.15	2.30	0.50	0.57
	2 to 4	10	0.15	7.83	1.25	2.37	3	0.20	1.00	0.52	0.43
	0 to 2	1	0.38	0.38	0.38	.	.	.	.	.	.
	Total	41	0.13	7.83	0.70	1.38	44	0.10	2.30	0.39	0.35
USU	2 to 4	2	0.30	6.69	3.50	4.52	10	0.20	5.30	1.23	1.65
	0 to 2	11	0.15	2.94	0.65	0.86	12	0.20	57.30	6.28	16.24
	-2 to 0	11	0.18	8.56	2.27	3.13	13	0.15	42.70	10.49	15.72
	-4 to -2	13	0.20	7.40	0.94	1.95	13	0.15	44.80	5.59	13.39
	-6 to -4	12	0.21	8.71	1.89	2.57	13	0.15	39.30	5.13	12.34
	-8 to -6	12	0.25	28.48	3.71	8.05	13	0.15	83.60	8.55	23.19
	-10 to -8	13	0.74	114.31	16.49	31.41	14	0.15	14.70	1.75	4.05
	-12 to -10	14	1.33	240.81	70.76	93.31	13	0.20	246.70	26.03	70.59
	-14 to -12	12	11.63	4412.37	727.60	1563.26	12	0.20	31.00	3.06	8.82
	-16 to -14	10	57.93	3798.38	518.42	1153.89	7	0.15	1.80	0.72	0.76
	-18 to -16	6	59.30	304.19	201.89	85.59	.	.	.	.	.
	Total	116	0.15	4412.37	141.81	632.82	120	0.15	246.70	7.33	26.46
MFGU	-14 to -12	1	3033.83	3033.83	3033.83	.	1	2261.90	2261.90	2261.90	.
	-16 to -14	2	6898.91	13323.58	10111.24	4542.92	5	3.60	9726.77	1948.95	4347.93
	-18 to -16	7	65.10	17029.53	2798.69	6291.82	13	0.20	390.90	55.47	113.84
	-20 to -18	14	191.64	2261.17	488.48	520.49	15	0.20	4200.90	528.16	1335.90
	-22 to -20	10	137.28	30056.10	3288.71	9406.06	10	0.20	288.32	74.66	113.85
	-24 to -22	12	56.54	331.59	179.64	102.19	8	0.20	8.50	2.20	2.82
	-26 to -24	5	23.41	201.95	121.61	76.42	4	0.20	36.50	12.51	17.10
	-28 to -26	3	7.31	226.99	121.81	110.13	1	0.20	0.20	0.20	.
	-30 to -28	1	13.15	13.15	13.15	.	.	.	.	.	.
	Total	55	7.31	30056.10	1558.46	4916.03	57	0.20	9726.77	376.57	1471.04
LSU	-22 to -20	1	664.18	664.18	664.18	.	3	0.60	3887.58	2537.03	2198.15
	-24 to -22	2	19.52	8858.93	4439.23	6250.41	6	0.20	3279.60	798.48	1300.99
	-26 to -24	8	62.29	17686.46	4421.24	7446.19	10	0.20	4132.90	551.82	1301.99
	-28 to -26	10	95.48	11322.78	2479.58	3951.42	13	0.20	8313.75	976.92	2326.32
	-30 to -28	10	117.45	8374.13	2024.60	3194.20	14	0.30	1256.50	212.43	374.85
	-32 to -30	12	19.92	7397.80	1232.98	2289.02	13	0.20	583.10	63.21	157.71
	-34 to -32	13	6.75	8911.22	1883.02	3113.33	11	0.15	211.40	53.79	79.33
	-36 to -34	10	40.98	10456.12	2073.13	4030.31	9	0.20	857.60	189.68	323.49
	-38 to -36	6	48.87	8349.02	1521.04	3345.73	.	.	.	.	.
	Total	72	6.75	17686.46	2209.54	3943.33	79	0.15	8313.75	464.74	1260.41

A.1.2.4 Semivariogram Results

In this study, the computer software used to perform the geostatistical calculations was Battelle's BATGAM software, which is based on the GSLIB Software written by the Department of Applied Earth Sciences at Stanford University, and documented and released by Prof. Andre Journel and Dr. Clayton Deutsch (Deutsch and Journel, 1998). The primary subroutine used to calculate experimental semivariograms was GAMV3, which is used for three-dimensional irregularly spaced data.

For the three-dimensional spatial analyses, horizontal separation distance classes were defined in increments of 5 ft. with a tolerance of 2.5 ft., while vertical distances were defined in increments of 2 ft. with a tolerance of 1 ft. Horizontal separation directions were defined, after rotation 30º west from North (see Figures A.1-2 and A.1-3), in the four primary directions of north, northeast, east, and southeast with a tolerance of 22.5º.

Data were analyzed separately for the Resistive Heating and ISCO plots, and vertically the data were considered separately by layer (i.e., USU, MFGU and LSU layers). Semivariogram and kriging analyses were not performed with the vadose data since the pre-remediation TCE concentrations were already relatively low and insignificant. Results from the semivariogram analyses are presented in Figures A.1-4 to A.1-15, as well as Table A.1-5. The key points indicated in the semivariogram analysis results are as follows:

(a) For all experimental semivariograms calculated with the TCE data, no horizontal directional differences (i.e., anisotropies) were observed; however, strong anisotropy for the horizontal versus vertical directions was often observed. Therefore, in Figures 3 through 14 the omni-directional horizontal semivariogram (experimental and model) is shown along with the vertical semivariogram (experimental and model).

(b) In all cases, the experimental semivariograms are relatively variable due to high data variability and modest sample sizes. As a result, the semivariogram model fitting is relatively uncertain, meaning that a relatively wide range of semivariogram models could adequately fit the experimental semivariogram points. This probably does not affect the TCE estimates (especially the global estimates), but could significantly affect the associated confidence bounds.

(c) The models shown in Figures 3 through 14 are all gaussian semivariogram models, chosen to be consistent with the experimental semivariogram shapes found for all twelve TCE data sets at this Cape Canaveral site. The fitted semivariograms model parameters are listed in Table 5.

Table A.1-5. Fitted Semivariogram Model Parameters for TCE at Cape Canaveral

	Data Set			Semivariogram				
Figure No.	**Plot**	**Layer**	**Pre- or Post-Remediation**	**Gaussian Type**	**Nugget Var. $(mg/kg)^2$**	**Total Sill Var. $(mg/kg)^2$**	**Omni-Horizontal Range (ft.)**	**Vertical Range (ft.)**
3	Resistive Heating	USU	PRE	Anisotropic	6.0×10^3	6.4×10^4	23	3
4	Resistive Heating	USU	POST	Anisotropic	2.0×10^4	1.9×10^5	35	3
5	Resistive Heating	MFGU	PRE	Anisotropic	1.0×10^6	2.0×10^7	35	5
6	Resistive Heating	MFGU	POST	Anisotropic	5.0×10^4	6.0×10^5	35	5
7	Resistive Heating	LSU	PRE	Isotropic	2.5×10^7	8.5×10^7	9	9
8	Resistive Heating	LSU	POST	Anisotropic	4.0×10^3	2.0×10^4	23	3
9	ISCO	USU	PRE	Anisotropic	5.0×10^4	3.0×10^5	12	3
10	ISCO	USU	POST	Isotropic	5.0×10^1	4.0×10^2	3	3
11	ISCO	MFGU	PRE	Anisotropic	2.5×10^6	2.0×10^7	35	3
12	ISCO	MFGU	POST	Anisotropic	2.0×10^5	1.4×10^6	52	3
13	ISCO	LSU	PRE	Anisotropic	1.0×10^6	1.0×10^7	23	3
14	ISCO	LSU	POST	Anisotropic	7.0×10^4	6.7×10^5	35	3

A.1.2.5 Kriging Results

The kriging analysis was performed using the BATGAM software and GSLIB subroutine KT3D. To conduct this analysis, each plot was defined as a set of vertical layers and sub-layers. Estimated mean TCE concentrations were then calculated via kriging for each sub-layer separately, as well as across the sub-layers. The vertical layering for kriging was consistent with the semivariogram modeling:

(a) Kriging the Resistive Heating plot was performed separately for the USU, MFGU and LSU layers. The USU layer was sub-divided into 11 two-foot sub-layers extending across elevations from –20 to +2 ft. The MFGU layer was sub-divided into 10 two-foot sub-layers extending across elevations from –32 to –12 ft. The LSU layer was sub-divided into 11 two-foot sub-layers from elevations of –40 to –18 ft.

(b) Kriging of the ISCO plot was also done separately for the USU, MFGU and LSU layers. The USU layer consisted of 11 two-foot sub-layers across elevations from –18 to +4 ft. The MFGU layer consisted of 9 sub-layers across elevations from –30 to –12 ft. The LSU layer consisted of 9 sub-layers across elevations from –38 to –20 ft.

(c) For kriging of the two-foot sub-layers, the data search was restricted to consider only three sub-layers, the current sub-layer and that immediately above and below. The data search was not restricted horizontally.

(d) For kriging of an entire layer (i.e., USU or MFGU or LSU separately), the data search considered all available data at all elevations. Note that by extending the data search radius to include all data within a plot, an implicit assumption is made that the semivariogram model holds true for distances up to about 100 ft., which are distances beyond those observable with this dataset in the experimental semivariograms. This assumption seems reasonable given the relatively short dimensions of the Resistive Heating and ISCO plots.

Results from the kriging analysis are presented in Tables A.1-6 and A.1-7 for the Resistive Heating and ISCO pre- and post-remediation data, and for each of USU, MFGU and LSU layers, as well as by sub-layer within each layer. Because of the shortcomings of using the ordinary kriging variance (discussed in Section 1.0) for local estimates, confidence bounds are only presented in Tables 6 and 7 for the global layer estimates (shaded rows). In cases where the upper confidence bound for the post-remediation average TCE concentration falls below the lower confidence bound for the pre-remediation average TCE concentration, the post-remediation TCE concentrations are statistically significantly lower than the pre-remediation TCE concentrations (denoted with a * in the tables). The estimated TCE reductions, expressed on a percentage basis, are also shown in Tables A.1-6 and A.1-7 and generally (with the exception of the TCE increase in the Resistive Heating USU layer) vary between 70% and 96%, based on the global estimates.

Table A.1-8 shows how the TCE concentration estimates (average, lower bound, and upper bound as determined in Table A.1-7) for ISCO plot are weighted and converted into TCE masses. The concentration estimates in the three stratigraphic units are multiplied by the number of grid cells sampled (N) in each stratigraphic unit and the mass of dry soil in each cell (26,831.25 kg). The mass of soil in each grid cell is the volume of each 18.75 ft x 16.67 ft x 2 ft grid cell (the area of the plot divided into a 4 x 3 grid; the thickness of each grid cell is 2 ft).

Table A.1-6. Kriging Results for TCE in the Resistive Heating Plot

Layer	Feet Above Sea Level (MSL)	Pre-Remediation TCE (mg/kg)	Post-Remediation TCE (mg/kg) / Percent Reduction
USU	0 to 2	3	32
	-2 to 0	2	21
	-4 to -2	2	18
	-6 to -4	1	32
	-8 to -6	14	46
	-10 to -8	31	297
	-12 to -10	124	325
	-14 to -12	118	122
	-16 to -14	182	78
	-18 to -16	245	61
	-20 to -18	88	41
	Total	64	112 / -75%
	95% C.I.	(19, 110)	(38, 186)
	90% C.I.	(26, 103)	(49, 174)
	80% C.I.	(34, 94)	(63, 160)
MFGU	-14 to -12	.	1450
	-16 to -14	412	606
	-18 to -16	1375	635
	-20 to -18	2125	478
	-22 to -20	1765	181
	-24 to -22	1419	119
	-26 to -24	2809	54
	-28 to -26	1705	12
	-30 to -28	1	3
	-32 to -30	1	.
	Total	1655	408 / 75%
	95% C.I.	(251, 3059)	(165, 650)
	90% C.I.	(473, 2837)	(204, 612)
	80% C.I.	(731, 2579)	(248, 567)*
LSU	-20 to -18	.	512
	-22 to -20	140	204
	-24 to -22	151	166
	-26 to -24	207	180
	-28 to -26	2394	239
	-30 to -28	2462	189
	-32 to -30	2246	135
	-34 to -32	3190	153
	-36 to -34	7241	154
	-38 to -36	8225	118
	-40 to -38	5615	.
	Total	4092	183 / 96%
	95% C.I.	(1463, 6721)	(154, 212)*
	90% C.I.	(1879, 6305)	(159, 208)*
	80% C.I.	(2362, 5822)	(164, 202)*

* TCE reduction is statistically significant.

Table A.1-7. Kriging Results for TCE in the ISCO Plot

Layer	Feet Above Sea Level (MSL)	Pre-Remediation TCE (mg/kg)	Post-Remediation TCE (mg/kg) / Percent Reduction
USU	2 to 4	2	1
	0 to 2	1	5
	-2 to 0	1	6
	-4 to -2	2	7
	-6 to -4	3	9
	-8 to -6	9	5
	-10 to -8	31	12
	-12 to -10	53	16
	-14 to -12	613	6
	-16 to -14	760	4
	-18 to -16	167	.
	Total	146	8 / 95%
	95% C.I.	(45, 246)	(4, 11)*
	90% C.I.	(61, 230)	(4, 11)*
	80% C.I.	(80, 212)	(5, 10)*
MFGU	-14 to –12	7963	3593
	-16 to –14	9414	1501
	-18 to –16	2684	135
	-20 to -18	1508	619
	-22 to -20	2655	196
	-24 to -22	220	30
	-26 to -24	150	8
	-28 to -26	97	.
	-30 to -28	71	.
	Total	1922	570 / 70%
	95% C.I.	(712, 3133)	(230, 909)
	90% C.I.	(903, 2942)	(284, 856)*
	80% C.I.	(1126, 2719)	(346, 793)*
LSU	-22 to -20	4665	2021
	-24 to -22	10048	954
	-26 to -24	4796	846
	-28 to -26	2036	823
	-30 to -28	1876	245
	-32 to -30	1780	102
	-34 to -32	1453	73
	-36 to -34	1972	183
	-38 to -36	2491	.
	Total	2282	486 / 79%
	95% C.I.	(1578, 2986)	(311, 660)*
	90% C.I.	(1690, 2875)	(339, 632)*
	80% C.I.	(1819, 2746)	(371, 600)*

* TCE reduction is statistically significant.

Table A.1-8. Calculating Total TCE Masses based on TCE Average Concentrations and Upper and Lower Bounds

ISCO Plot Geology Units	Pre-Demonstration							Post-Demonstration						
		TCE Concentration			TCE Mass *				TCE Concentration			TCE Mass *		
	N	Average (mg/kg)	Lower Bound (mg/kg)	Upper Bound (mg/kg)	Average (kg)	Lower Bound (kg)	Upper Bound (kg)	N	Average (mg/kg)	Lower Bound (mg/kg)	Upper Bound (mg/kg)	Average (kg)	Lower Bound (kg)	Upper Bound (kg)
Upper Sand Unit	116	146	80	212	454	250	659	120	8	5	10	26	18	34
Middle Fine-Grained Unit	55	1,922	1,126	2,719	2,836	1,668	4,005	57	570	346	793	872	532	1,211
Lower Sand Unit	72	2,282	1,819	2,746	4,408	3,519	5,298	79	486	371	600	1,030	788	1,272
Total ISCO Plot	243	-	-	-	7,699	6,217	9,182	256	-	-	-	1,928	1,511	2,345

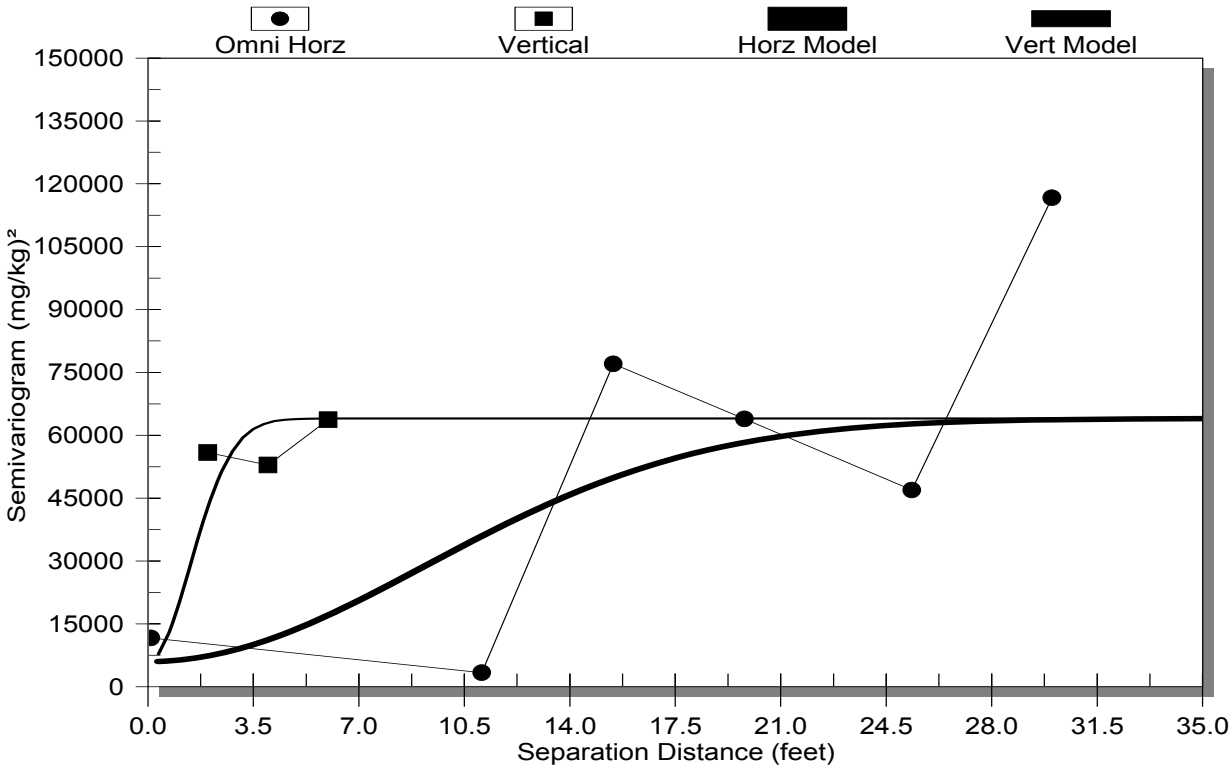

Figure A.1-4. Pre-Remediation TCE Semivariograms for Resistive Heating Plot and USU

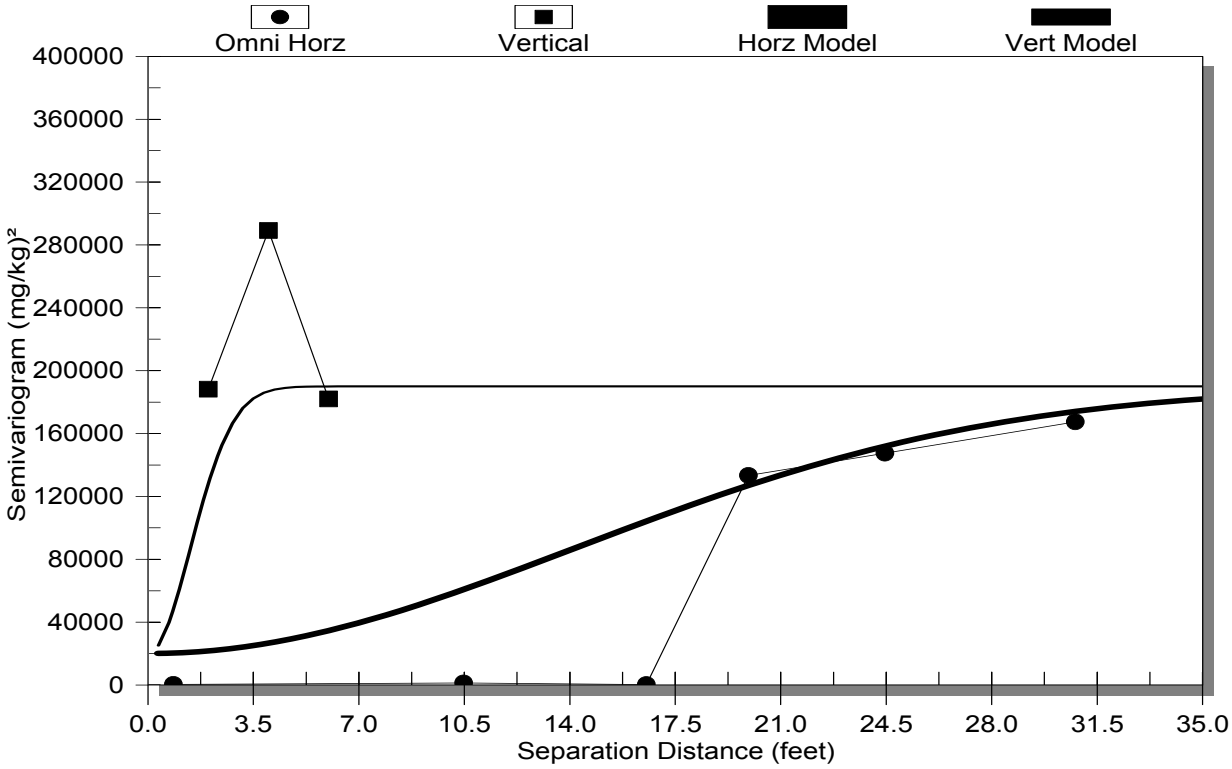

Figure A.1-5. Post-Remediation TCE Semivariograms for Resistive Heating Plot and USU

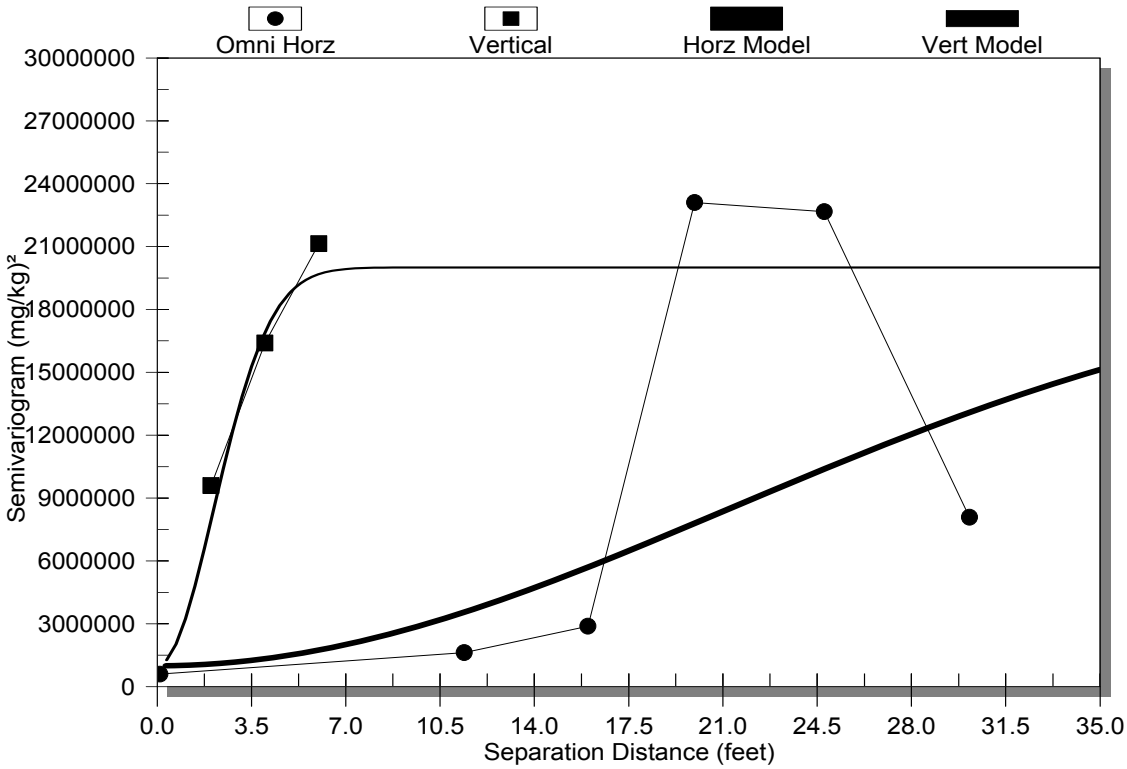

Figure A.1-6. Pre-Remediation TCE Semivariograms for Resistive Heating Plot and MFGU

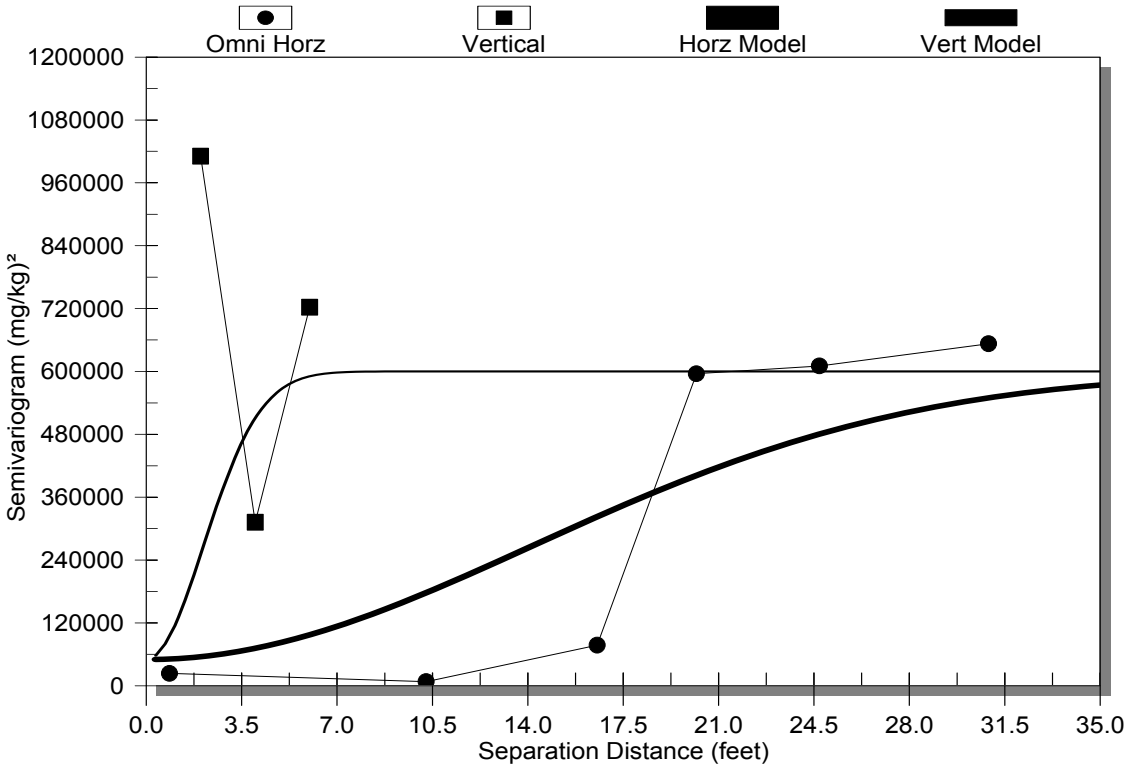

Figure A.1-7. Post-Remediation TCE Semivariograms for Resistive Heating Plot and MFGU

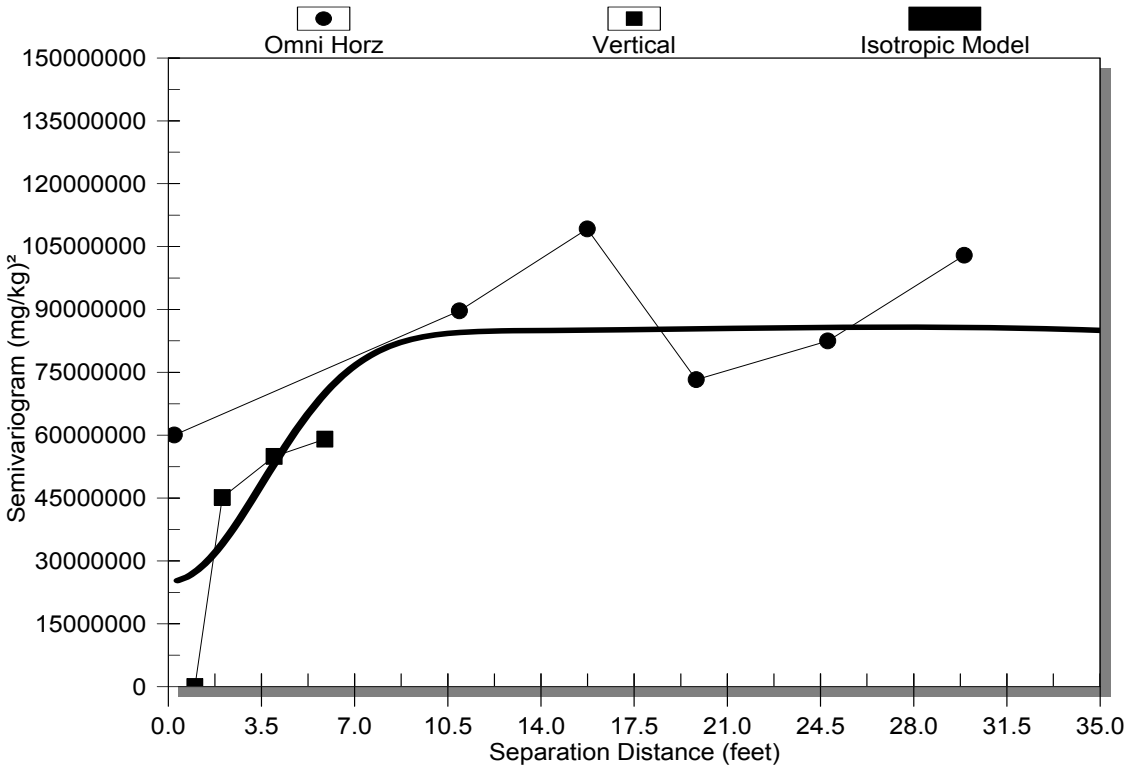

Figure A.1-8. Pre-Remediation TCE Semivariograms for Resistive Heating Plot and LSU

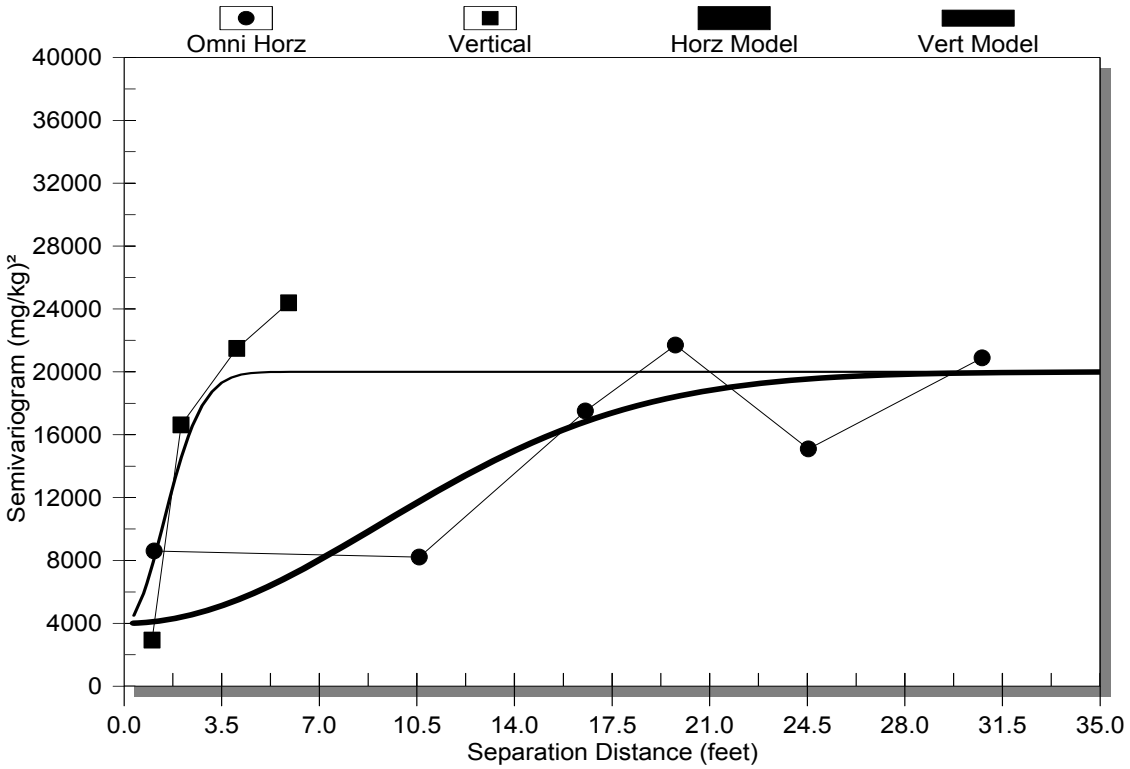

Figure A.1-9. Post-Remediation TCE Semivariograms for Resistive Heating Plot and LSU

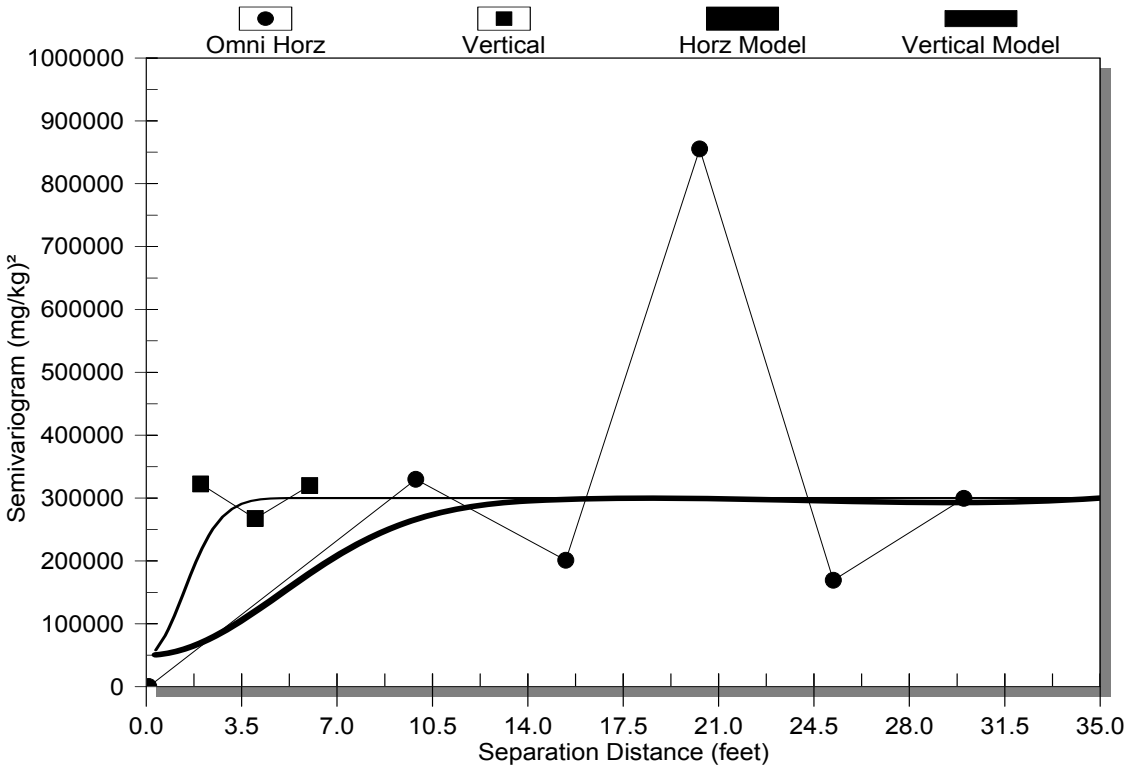

Figure A.1-10. Pre-Remediation TCE Semivariograms for ISCO Plot and USU

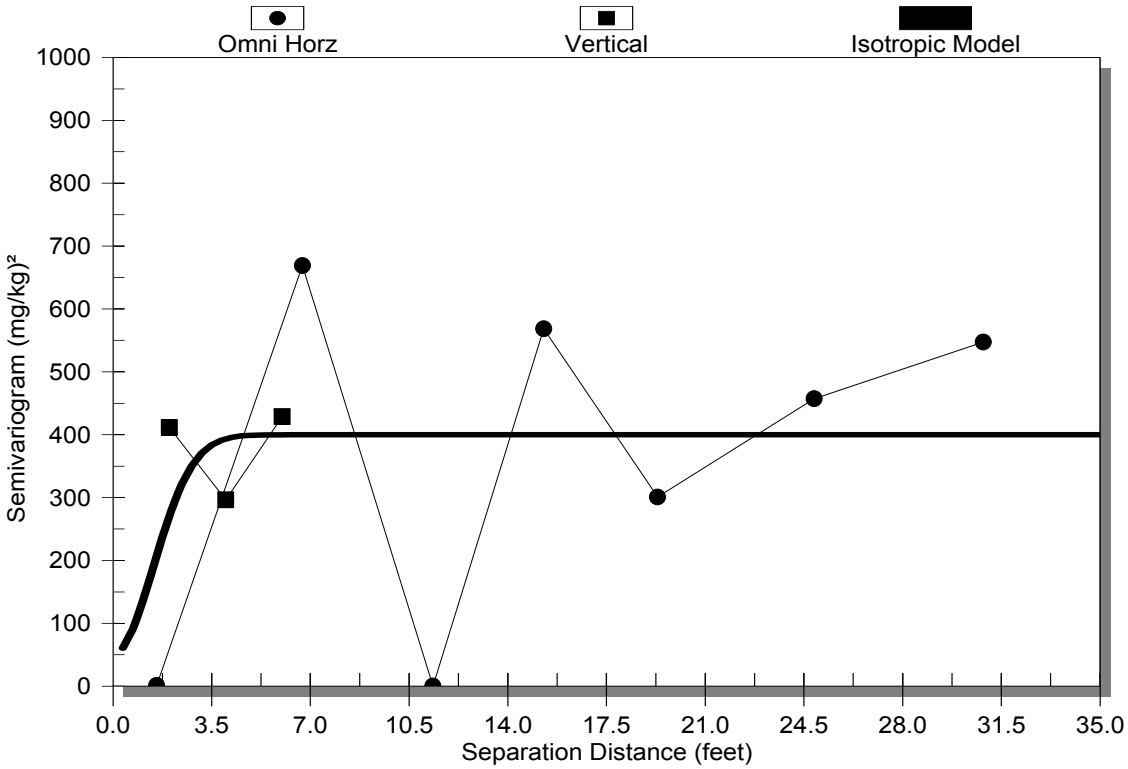

Figure A.1-11. Post-Remediation TCE Semivariograms for ISCO Plot and USU

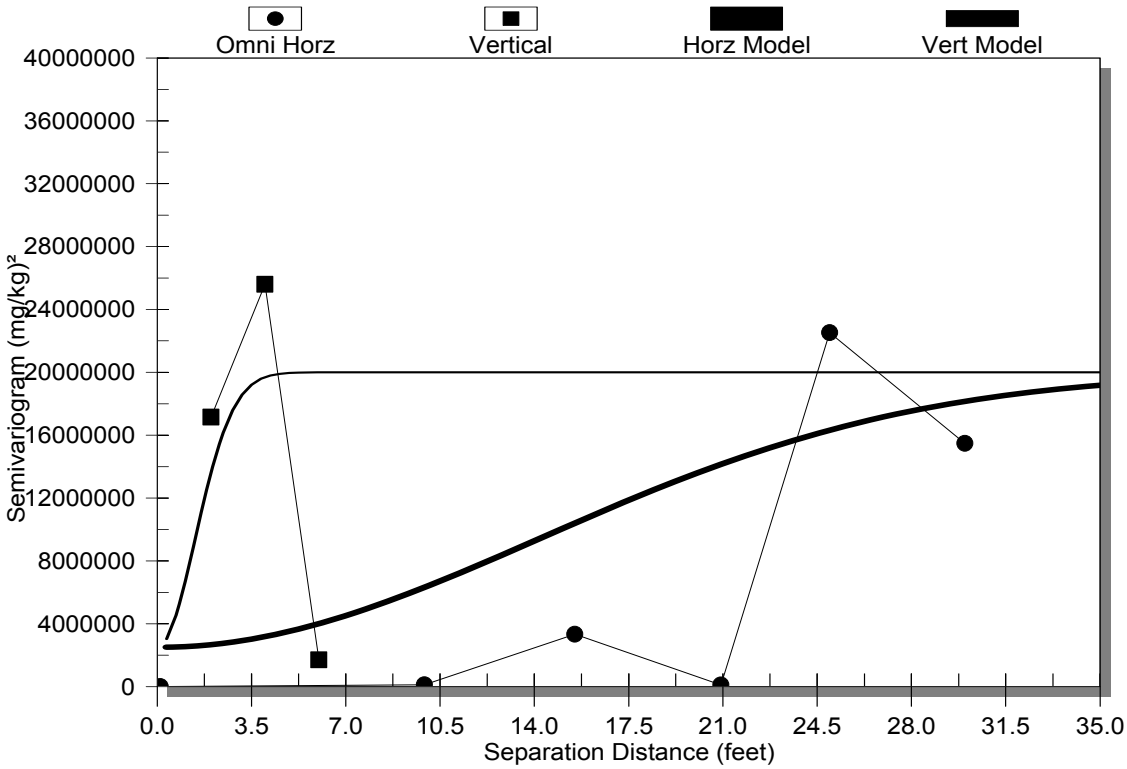

Figure A.1-12. Pre-Remediation TCE Semivariograms for ISCO Plot and MFGU

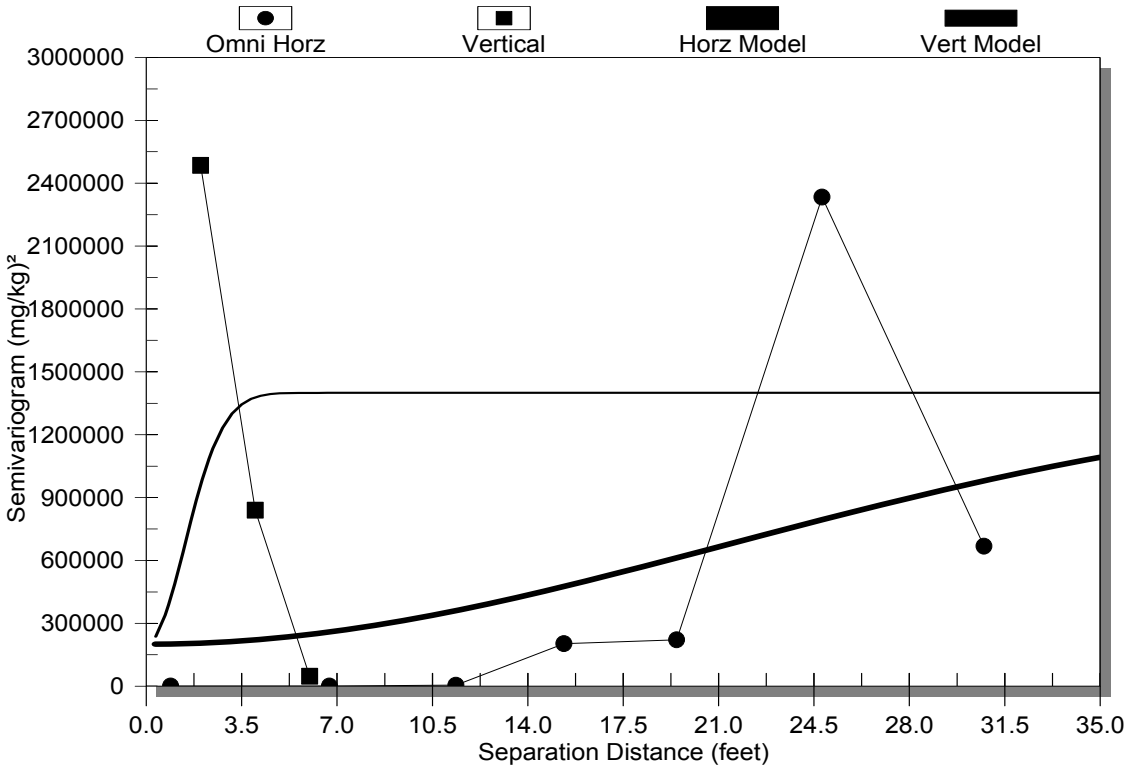

Figure A.1-13. Post-Remediation TCE Semivariograms for ISCO Plot and MFGU

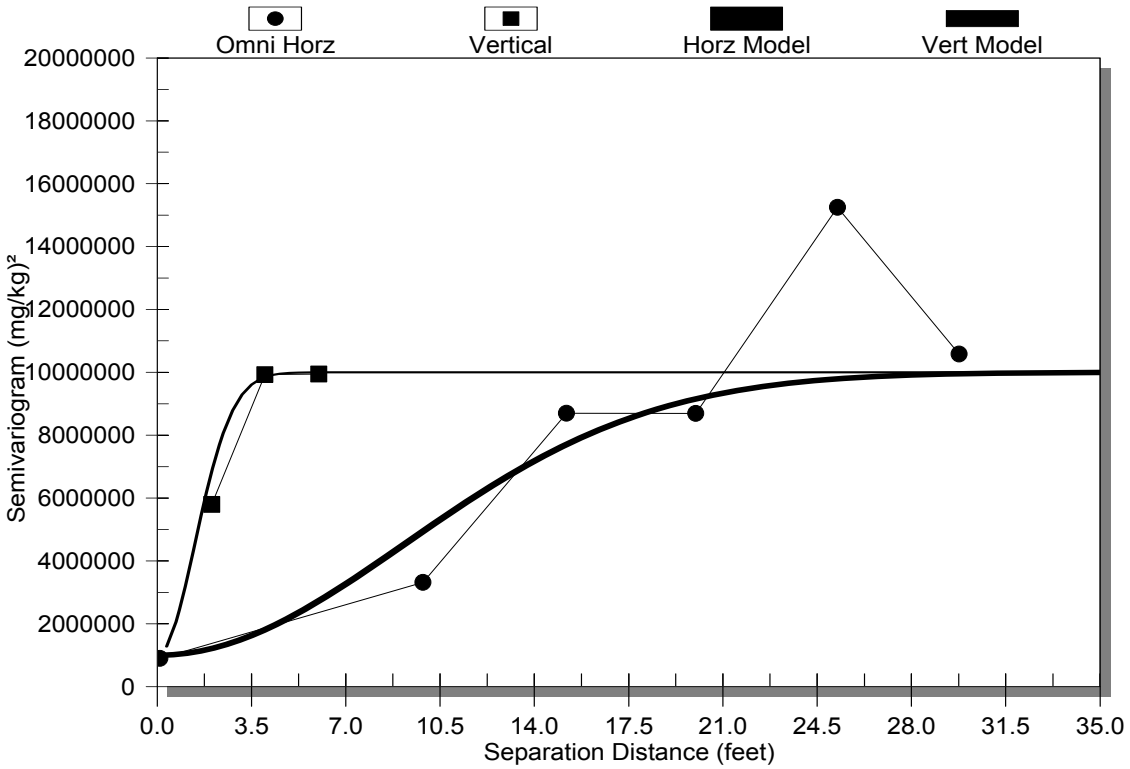

Figure A.1-14. Pre-Remediation TCE Semivariograms for ISCO Plot and LSU

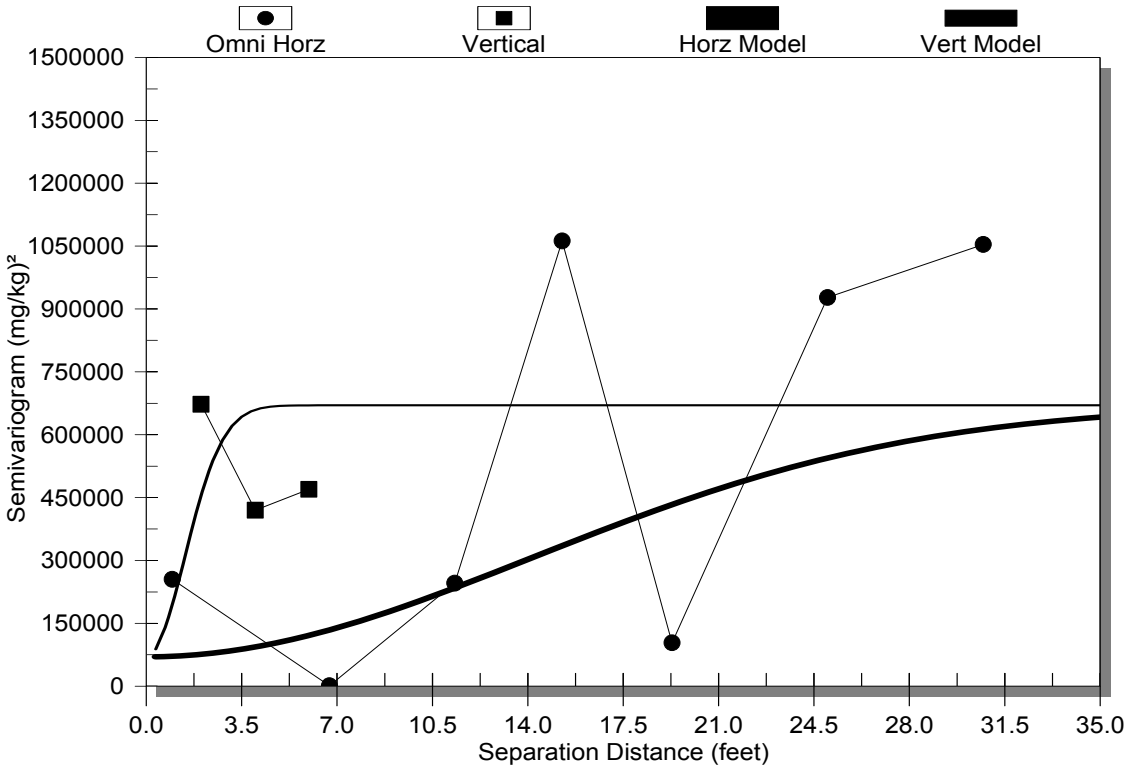

Figure A.1-15. Post-Remediation TCE Semivariograms for ISCO Plot and LSU

A.2 Sample Collection and Extraction Methods

This section describes the modification made to the EPA standard methods to address the lithologic heterogeneities and extreme variability of the contaminant distribution expected in the DNAPL source region at Launch Complex 34. Horizontal variability was addressed by collecting a statistically determined number (12) of soil cores in the ISCO Plot. The vertical variability at each soil coring location was addressed with this modified sampling and extraction procedure, which involved extraction of much larger quantities of soil in each extracted sample, as well as allowed collection and extraction of around 300 samples in the field per event. This extraction allowed the extraction and analysis of the entire vertical column of soil at a given coring location.

A.2.1 Soil Sample Collection (Modified ASTM D4547-91) (1997b)

The soil samples collected before and after the demonstration were sampled using a stainless steel sleeve driven into the subsurface by a cone penetrometer test (CPT) rig. After the sleeve had been driven the required distance, it was brought to the surface and the soil sample was examined and characterized for lithology. One quarter of the sample was sliced from the core and placed into a pre-weighed 500-mL polyethylene container. At locations where a field duplicate sample was collected, a second one-quarter sample was split from the core and placed into another pre-weighed 500-mL polyethylene container. The remaining portion of the core was placed into a 55-gallon drum and disposed of as waste. The samples were labeled with the date, time, and sample identification code, and stored on ice at 4°C until they were brought inside to the on-site laboratory for the extraction procedure.

After receiving the samples from the drilling activities, personnel staffing the field laboratory performed the methanol extraction procedure as outlined in Section A.2.2 of this appendix. The amount of methanol used to perform the extraction technique was 250 mL. The extraction procedure was performed on all of the primary samples collected during drilling activities and on 5% of the field duplicate samples collected for quality assurance. Samples were stored at 4°C until extraction procedures were performed. After the extraction procedure was finished, the soil samples were dried in an oven at 105°C and the dry weight of each sample was determined. The samples were then disposed of as waste. The remaining three-quarter section of each core previously stored in a separate 500-mL polyethylene bottle were archived until the off-site laboratory had completed the analysis of the methanol extract. The samples were then disposed of in an appropriate manner.

A.2.2 Soil Extraction Procedure (Modified EPA SW846-Method 5035)

After the soil samples were collected from the drilling operations, samples were placed in pre-labeled and pre-weighed 500-mL polyethylene containers with methanol and then stored in a refrigerator at 4°C until the extraction procedure was performed. Extraction procedures were performed on all of the "A" samples from the outdoor and indoor soil sampling. Extraction procedures also were performed on 5% of the duplicate (or "B") samples to provide adequate quality assurance/quality control (QA/QC) on the extraction technique.

Extreme care was taken to minimize the disturbance of the soil sample so that loss of volatile components was minimal. Nitrile gloves were worn by field personnel whenever handling sample cores or pre-weighed sample containers. A modification of EPA SW846-Method 5035 was used to procure the cored samples in the field. Method 5035 lists different procedures for processing samples that are expected to contain low concentrations (0.5 to 200 μg/kg) or high concentrations

(>200 µg/kg) of volatile organic compounds (VOCs). Procedures for high levels of VOCs were used in the field because those procedures facilitated the processing of large-volume sample cores collected during soil sampling activities.

Two sample collection options and corresponding sample purging procedures are described in Method 5035; however, the procedure chosen for this study was based on collecting approximately 150 to 200 g of wet soil sample in a pre-weighed bottle that contains 250 mL of methanol. A modification of this method was used in the study, as described by the following procedure:

- The 150 to 200 g wet soil sample was collected and placed in a pre-weighed 500 mL polypropylene bottle. After capping, the bottle was reweighed to determine the wet weight of the soil. The container was then filled with 250 ml of reagent grade methanol. The bottle was weighed a third time to determine the weight of the methanol added. The bottle was marked with the location and the depth at which the sample was collected.

- After the containers were filled with methanol and the soil sample they were placed on an orbital shaker table and agitated for approximately 30 min.

- Containers were removed from the shaker table and reweighed to ensure that no methanol was lost during the agitation period. The containers were then placed upright and suspended soil matter was allowed to settle for approximately 15 min.

- The 500 mL containers were then placed in a floor-mounted centrifuge. The centrifuge speed was set at 3,000 rpm and the samples were centrifuged for 10 min.

- Methanol extract was then decanted into disposable 20-mL glass volatile organic analysis (VOA) vials using 10-mL disposable pipettes. The 20-mL glass VOA vials containing the extract then were capped, labeled, and stored in a refrigerator at 4°C until they were shipped on ice to the analytical laboratory.

- Methanol samples in VOA vials were placed in ice chests and maintained at approximately 4°C with ice. Samples were then shipped with properly completed chain-of-custody forms and custody seals to the subcontracted off-site laboratory.

- The dry weight of each of the soil samples was determined gravimetrically after decanting the remaining solvent and drying the soil in an oven at 105°C. Final concentrations of VOCs were calculated per the dry weight of soil.

Three potential concerns existed with the modified solvent extraction method. The first concern was that the United States Environmental Protection Agency (U.S. EPA) had not formally evaluated the use of methanol as a preservative for VOCs. However, methanol extraction often is used in site characterization studies, so the uncertainty in using this approach was reasonable. The second concern was that the extraction procedure itself would introduce a significant dilution factor that could raise the method quantitation limit beyond that of a direct purge-and-trap procedure. The third concern was that excess methanol used in the extractions would likely fail the ignitability characteristic, thereby making the unused sample volume a hazardous waste. During characterization activities, the used methanol extract was disposed of as hazardous waste into a 55-gallon drum. This methanol extraction method was tested during preliminary site characterization activities at this site (see Appendix G, Table G-1) and, after a few refinements,

was found to perform acceptably in terms of matrix spike recoveries. Spiked TCE recoveries in replicate samples ranged from 72 to 86%.

The analytical portion of Method 5035 describes a closed-system purge-and-trap process for use on solid media such as soils, sediments, and solid waste. The purge-and-trap system consists of a unit that automatically adds water, surrogates, and internals standards to a vial containing the sample. Then the process purges the VOCs using an inert gas stream while agitating the contents of the vial, and finally traps the released VOCs for subsequent desorption into a gas chromatograph (GC). STL Environmental Services performed the analysis of the solvent extraction samples. Soil samples were analyzed for organic constituents according to the parameters summarized in Table A.2-1. Laboratory instruments were calibrated for VOCs listed under U.S. EPA Method 601 and 602. Samples were analyzed as soon as was practical and within the designated holding time from collection (14 days). No samples were analyzed outside of the designated 14-day holding time.

Table A.2-1. Soil Sampling and Analytical Parameters

Analytes	Extraction Method	Analytical Method	Sample Holding Time	Matrix
VOCs[(a)]	SW846-5035	SW846-8260	14 days	Methanol

(a) EPA 601/602 list.

A.3 List of Standard Sample Collection and Analytical Methods

Table A.3-1. Sample Collection Procedures

Measurements	Task/Sample Collection Method	Equipment Used
Primary Measurements		
CVOCs	Soil sampling/ Mod.[(a)] ASTM D4547-98 (1997c)	Stainless steel sleeve 500-mL plastic bottle
CVOCs	Groundwater sampling/ Mod.[(a)] ASTM D4448-01 (1997a)	Peristaltic pump Teflon™ tubing
Secondary Measurements		
TOC	Soil sampling/ Mod.[(a)] ASTM D4547-91 (1997c)	Stainless steel sleeve
Field parameters[(b)] TOC BOD Inorganics–cations Inorganics–anions TDS Alkalinity	Groundwater sampling/ Mod.[(a)] ASTM D4448-01 (1997a)	Peristaltic pump Teflon™ tubing
Hydraulic conductivity	Hydraulic conductivity/ ASTM D4044-96 (1997d)	Winsitu® troll Laptop computer
Groundwater level	Water levels	Water level indicator
CVOCs	Vapor Sampling/Tedlar Bag, TO-14	Vacuum Pump

(a) Modifications to ASTM are detailed in Appendix B.
(b) Field parameters include pH, ORP, temperature, DO, and conductivity. A flowthrough well will be attached to the peristaltic pump when measuring field parameters.
ASTM = American Society for Testing and Materials.

Table A.3-2. Sample Handling and Analytical Procedures

Measurements	Matrix	Amount Collected	Analytical Method	Maximum Holding Time[a]	Sample Preservation[b]	Sample Container	Sample Type
Primary Measurements							
CVOCs	Soil	250 g	Mod. EPA 8260[c]	14 days	4°C	Plastic	Grab
CVOCs	Groundwater	40-mL × 3	EPA 8260[d]	14 days	4°C, pH < 2 HCl	Glass	Grab
Secondary Measurements							
CVOCs	Groundwater	40-mL × 3	EPA 8021/8260[d]	14 days	4°C, pH < 2 HCl	Glass	Grab
CVOCs	Vapor	1 L	TO-14	14 days	NA	Tedlar™ Bag	Grab
pH	Soil	50 g	Mod. EPA 9045c	7 days	None	Plastic	Grab
pH	Groundwater	50 mL	EPA 150.1	1 hour	None	Plastic	Grab
TOC	Soil	20 g	SW 9060	28 days	None	Plastic	Grab
TOC	Groundwater	125 mL	EPA 415.1	28 days	4°C, pH < 2 H_2SO_4	Plastic	Grab
BOD	Groundwater	1,000 mL	EPA 405.1	48 hours	4°C	Plastic	Grab
Hydraulic conductivity	Aquifer	NA	ASTM D4044-96 (1997d)	NA	NA	NA	NA
Inorganics–cations[e]	Groundwater	100 mL	SW 6010	28 days	4°C, pH<2, HNO3	Plastic	Grab
Inorganics–anions[e]	Groundwater	50 mL	EPA 300.0	28 days	4°C	Plastic	Grab
TDS	Groundwater	500 mL	EPA 160.1	7 days	4°C	Plastic	Grab
Alkalinity	Groundwater	200 mL	EPA 310.1	14 days	4°C	Plastic	Grab
Water levels	Aquifer	NA	Water level from the top of well casing	NA	NA	NA	NA

(a) Samples will be analyzed as soon as possible after collection. The times listed are the maximum holding times which samples will be held before analysis and still be considered valid. All data obtained beyond the maximum holding times will be flagged.

(b) Samples will be preserved immediately upon sample collection, if required.

(c) Samples will be extracted using methanol on site. For the detailed extraction procedure see Appendix B.

(d) The off-site laboratory will use EPA 8260.

(e) Cations include Ca, Mg, Fe, Mn, Na, and K. Anions include Cl, SO_4, and NO_3/ NO_2.

HCl = Hydrochloric acid.

NA = Not applicable.